THE BELL SYSTEM TECHNICAL JOURNAL
Vol. 58, No. 2, February 1979
Printed in U.S.A.

Imaging Reflector Arrangements to Form a Scanning Beam Using a Small Array

By C. DRAGONE and M. J. GANS

(Manuscript received May 23, 1978)

To obtain the performance of a large aperture phased array, a small phased array is combined with a large main reflector and an imaging arrangement of smaller reflectors to form a large image of the small array over the main reflector. An electronically scanable antenna with a large aperture is thus obtained, using a small array. An attractive feature of the imaging arrangement is that the main reflector need not be fabricated accurately, since small imperfections can be corrected efficiently by the array. As an application, a 4.2-m diameter antenna is discussed for a 12–14 GHz satellite with a field of view of 3 degrees by 6 degrees required for coverage of the continental United States.

I. INTRODUCTION

Use of a phased array in a satellite of large aperture diameter is proposed in Ref. 1 to form a narrow beam to communicate with ground stations in the United States. A large array in this case is not attractive, because of its weight and the loss and complexity of the long interconnections required by the large spacing between the array elements. Thus, we here propose the use of a small array combined with several reflectors as shown in Figs. 1 to 3. The reflectors are arranged so that a magnified image of the array S_0 is formed over the aperture of the main reflector. The magnification M relating the diameters D_0 and D_1 of the main reflector and the array, respectively, is chosen much greater than unity, i.e.,

$$M = \frac{D_0}{D_1} \gg 1, \tag{1}$$

so that the array is much smaller than the main reflector.

The main reflector S_0 in Figs. 1 and 2 may be difficult to fabricate accurately because of its large diameter. However, it is pointed out in

Section II that small imperfections are easily corrected because S_0 and the array are conjugate elements.* Another important property of the arrangements described here is that the transformation relating the field over the array aperture to the field over the main reflector aperture is essentially frequency independent, and therefore it can be approximated by its asymptotic behavior at high frequency. That is, the transformation can be determined accurately using the laws of geometric optics, as pointed out in Section II.

Use of several reflectors combined with a small array is not new. In particular, the Gregorian configuration of two confocal paraboloids shown in Fig. 1 is discussed in Refs. 2 and 3. In Ref. 3, the performance of this arrangement is analyzed by representing the field over the array aperture in terms of plane waves, and by then determining separately the transformation for each plane wave. Here, however, we shall see that our condition (3) allows the analysis to be carried out entirely using the laws of geometrical optics, as already pointed out. We first consider the arrangement of Fig. 1.

II. ANALYSIS

In Fig. 1, the first paraboloid, S_0, transforms a plane wave, propagating in the direction of the paraboloid axis, into a spherical wave converging toward the focus F. This spherical wave is then transformed into a plane wave, by the second paraboloid S_1, which is large enough to intercept all incident rays. After the second reflection, the reflected rays illuminate the array plane $\sum_1$. Since the illuminated area corresponds to the projection of the first paraboloid, its diameter D_1 is determined by D_0, and from Fig. 1,

$$M = \frac{D_0}{D_1} = \frac{f_0}{f_1}, \tag{2}$$

where f_1 and f_0 are the axial focal lengths of the two paraboloids. Thus, by choosing

$$\frac{f_0}{f_1} \gg 1,$$

a small array diameter D_1 is sufficient to intercept all the incident rays. Notice on $\sum_1$ the center of illumination is determined by the ray corresponding to the center C_0 of the paraboloid. The center C_1 of the array must therefore be placed on this ray, which will be called the *central ray*.

* Conjugate elements in an optical system have the property that the rays originating from a point of one element are transformed, by the optical system, into rays which pass through a corresponding point of the other element. Two such corresponding points are called conjugate points.

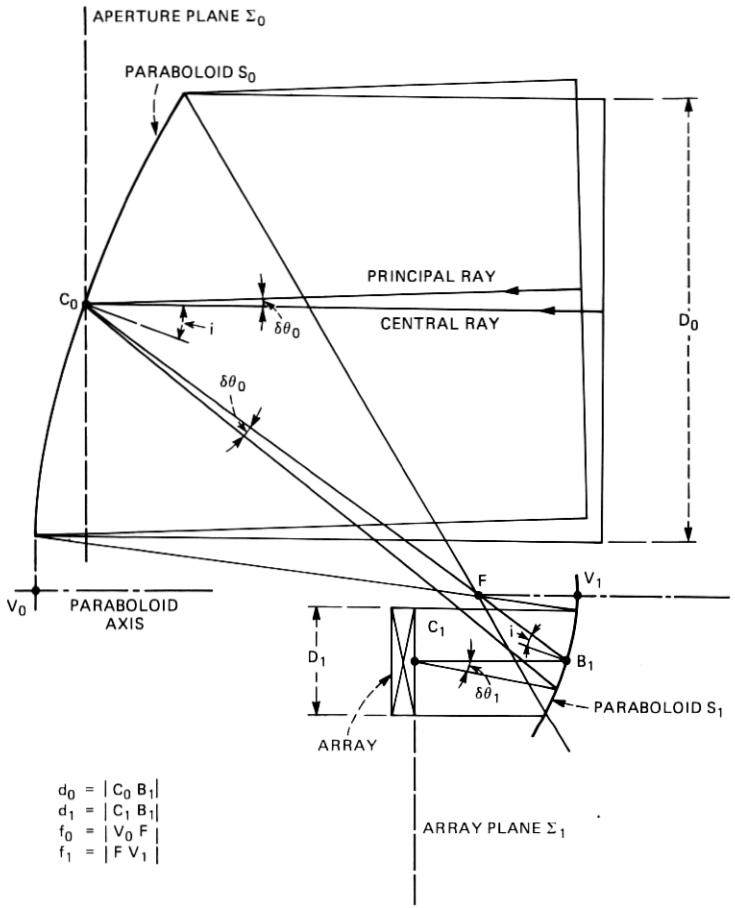

Fig. 1—A Gregorian arrangement of two confocal paraboloids magnifying a small array. The main reflector S_0 and the array are conjugate elements.

Now suppose in Fig. 1 the direction of the incident wave is changed so that the ray incident at C_0 makes a small angle $\delta\theta_0$ with respect to the central ray. The center of illumination will then vary with $\delta\theta_0$, unless C_0 and C_1 are conjugate points, as in Fig. 1. In this case, for small $\delta\theta_0$, all rays reflected at C_0 pass through C_1 after the second reflection. We thus conclude that, for maximum efficiency of illumination, the following condition must be satisfied:

> The center of the main reflector and the center of the array must be conjugate points. (3)

When this condition is satisfied, the field in the vicinity of C_1 is the image of the field in the vicinity of C_0. More precisely, let $\sum_0$ and $\sum_1$ be

the two planes orthogonal to the central ray, through C_0 and C_1. Then $\sum_0$ and $\sum_1$ are conjugate planes, in the vicinity of C_0 and C_1, and therefore the field E_1 on $\sum_1$ is the image of the field E_0 on $\sum_0$.

The consequences of this basic condition are now discussed. The transformation which relates the input field E_0 to the output field E_1 in Fig. 1 involves several reflections and, because of diffraction, the field propagating from one reflector to the next *cannot* be determined accurately using the laws of geometric optics. Thus, suppose Fresnel's diffraction formula is used to determine the transformation from one reflector to the other, or from the reflector to the array in Fig. 1. The details of such calculations are given in Ref. 4, where the general transformation between the input and output fields E_0 and E_1 of an optical system is derived. It is shown in Ref. 4 that, when the input and output planes are conjugate planes of the optical system, the output field E_1 is simply the image of the input field E_0, and it can be calculated using the laws of geometric optics. This result is quite remarkable for, in general, the laws of geometric optics give correctly only the field in the output plane, not the field inside the optical system. An important consequence of this result, which was used in Ref. 5 to obtain frequency independence in the far-field of a satellite antenna, is now pointed out.

Suppose in Fig. 1 the surface of the main reflector is not perfect, but it contains a small imperfection $\delta\ell$ causing a phase error $\delta\psi_0 \simeq 2k\delta\ell$ after reflection. Then, if P_0 is the location of the imperfection on the paraboloid, and P_1 is the corresponding point on the array plane, one has that E_1 will contain at P_1 a phase error $\delta\psi_1$ approximately equal to $\delta\psi_0$,

$$\delta\psi_1 \simeq 2k\delta\ell.$$

Since $\delta\ell$ is independent of frequency, the reflector deformation can be corrected by a frequency independent change in the time delay of the array element corresponding to P_1. This would not be true if C_0 and C_1 were not conjugate points.

Consider also the effect of a surface deformation on the subreflector in Fig. 1. Now, unless the subreflector and the array are conjugate elements, the resulting perturbation of E_1 will not be independent of $\delta\theta_0$, but its location will vary with $\delta\theta_0$. Furthermore, because of diffraction, E_1 will be perturbed both in amplitude and phase, and the perturbations will in general vary with frequency. Thus, surface deformations on the subreflector cannot be easily corrected.

2.1 Location of C_1

The location of C_1 is now determined. The ray reflected in Fig. 1 at C_0 for $\delta\theta_0 \neq 0$ will be called the principal ray. Let $\delta\theta_1$ be the angle this ray makes with the central ray at C_1. Then, since M is the magnification

of the two conjugate planes $\sum_0$ and $\sum_1$, the angles $\delta\theta_0$ and $\delta\theta_1$ must satisfy the well-known relation

$$\delta\theta_1 = M\delta\theta_0.$$

Now, from Fig. 1,

$$d_1\delta\theta_1 = d_0\delta\theta_0, \tag{4}$$

d_1 and d_0 being the distances of C_1 and C_0, respectively, from the center B_1 of the subreflector. One can show that

$$d_0 = \frac{f_1 + f_0}{\cos^2 i}, \tag{5}$$

i being the angle of incidence at C_0 (or B_1) for the central ray. From the above relations one obtains

$$d_1 = \frac{f_1 + f_0}{\cos^2 i}\frac{1}{M} \tag{6}$$

or

$$d_1 = \frac{f_1}{\cos^2 i}\quad\frac{M+1}{M} = |FB_1|\frac{M+1}{M}. \tag{7}$$

2.2 Use of an additional reflector to increase the distance d_1

In Fig. 1, the array is relatively close to the subreflector S_1, and this may be a disadvantage for some applications. In the application discussed in Section III, for instance, a greater distance d_1 will be needed to place a grid between the array and the subreflector for polarization or frequency diplexing. In this case, it is advantageous to use three reflectors S_0, S_0', and S_1 arranged as shown in Fig. 2.

To determine the distance $d_1 = |C_1B_1|$ between the array and the last reflector, which is a paraboloid, it is convenient to introduce the parameters ℓ, ξ_1, ξ_2, M_0 defined by

$$\ell = |C_0F'|$$

$$\frac{\ell}{\xi_1} = |B_0F'|$$

$$\frac{M_0\ell}{\xi_1} = |FB_0|$$

$$\frac{\ell}{\xi_2} = |B_1F|.$$

To determine the location of C_1 for small $\delta\theta_0$, consider in Fig. 2 the two rays reflected by the main paraboloid at C_0. One of the two rays is the central ray. Notice that the hyperboloid subreflector forms a

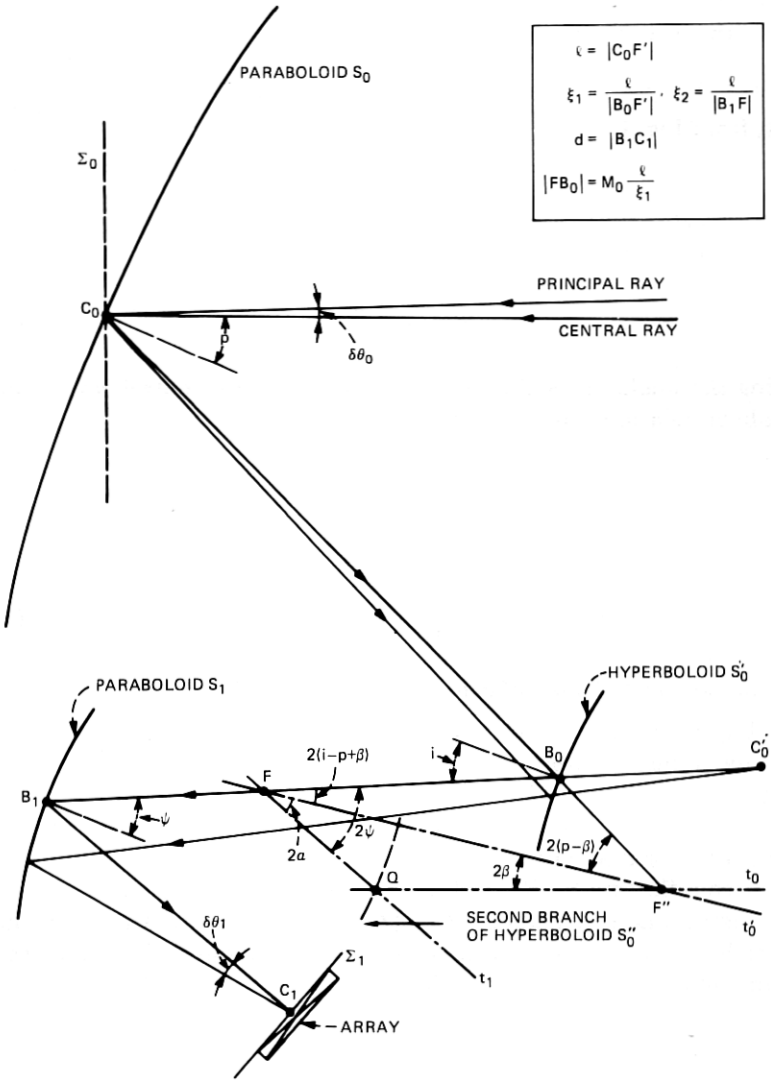

Fig. 2—Imaging arrangement of three reflectors.

virtual image C_0' of C_0. The last paraboloid subreflector transforms this virtual image into a real image C_1, where both rays meet after reflection by S_1

To determine the location of C_0', one has to find the paraxial focal length of the hyperboloid reflector. Taking into account that F' and F are conjugate points, whose distances from S_0' are ℓ/ξ_1 and $M_0\ell/\xi_1$,

respectively, the focal length in question is*

$$\frac{\ell}{\xi_1}\,\frac{M_0}{M_0-1}.$$

Thus, since the distance of C_0 from B_0 is

$$\ell\,\frac{\xi_1-1}{\xi_1},$$

using the lens equation one finds that the distance of C_0' from B_0 is

$$\ell\,M_0\,\frac{\xi_1-1}{\xi_1}\,\frac{1}{1+\xi_1(M_0-1)}.$$

The location of C_1 is next determined. The paraxial focal length of the last reflector S_1 is ℓ/ξ_2, and the distance of C_0' from B_1 is

$$\frac{\ell}{\xi_2}+\frac{\ell M_0^2}{1+\xi_1(M_0-1)}.$$

Therefore, using once more the lens equation, one finds for the distance of C_1 from B_1

$$d_1=\frac{\ell}{\xi_2}\left[1+\frac{1}{M_0^2}\,\frac{1+\xi_1(M_0-1)}{\xi_2}\right]. \tag{8}$$

One can verify that

$$M=\frac{D_0}{D_1}=M_0\xi_2, \tag{9}$$

which allows ξ_2 in eq. (8) to be expressed in terms of M and M_0, giving the result

$$d_1=\frac{\ell}{M}\left\{M_0+\frac{1}{M}\left[1+\xi_1(M_0-1)\right]\right\}. \tag{10}$$

This expression, which for $M_0=1$ can be shown to coincide with eq. (6), is a monotonic function of M_0. Thus, by choosing $M_0 >> 1$, as in Fig. 2, a distance d_1 appreciably greater than that of Fig. 1 is obtained.

An important difference between the two arrangements of Figs. 1 and 2 is that the various surfaces of revolution of the reflectors in Fig. 2 are not centered around the same axis, as in Fig. 1. In fact, in Fig. 2 the axis t_0' of the hyperboloid is tilted by the angles 2β and 2α, with respect to the axes t_0 and t_1 of the two paraboloids. This difference is now explained.

---

* According to the lens equation (Ref. 4), the inverse of the focal length must equal the sum of the inverses of the distances from the conjugate points to the reflector.

2.3 Orientation of the axes t_0, t'_0, t_1

For some applications, it is important that everywhere on the array plane the polarization of E_1 coincide with that of E_0. For $\delta\theta_0 = 0$, one can show this condition is satisfied in Fig. 1, provided the reflectors are centered around the same axis. In Fig. 2, on the other hand, either of the two angles α, β may be chosen arbitrarily provided the other angle satisfies the condition[6,7]

$$\tan \alpha = m \tan \beta, \tag{11}$$

where m is related to the eccentricity e of the hyperboloid through the relation

$$m = \frac{e+1}{e-1}. \tag{12}$$

It can be calculated once p, β, i are known, using the relation

$$m = \frac{\tan(p-\beta)}{\tan(i-p+\beta)}, \tag{13}$$

where the angles α, β, i, and p are as shown in Fig. 2.

Equation (11) has the following geometric significance. In Fig. 2, t_0 represents the axis of the main reflector, t'_0 the axis of the subreflector, and t_1 the axis of the imaging reflector. The reflector S'_0 is derived from one of the two branches of an hyperboloid. If S''_0 denotes the other branch, then it is shown in Ref. 7 that the point of intersection Q of the two axes t'_0 and t_1 must be a point of S''_0, as shown in Fig. 2. Then, since 2α and 2β can be interpreted as the angles the two focal radii FQ and $F'Q$ make with the axis t'_0 one obtains eq. (11).

From the triangle FB_0F' in Fig. 2, taking into account that $|FB_0| = M_0 |B_0F'|$, one has

$$\sin(2p - 2\beta) = M_0 \sin 2(i - p + \beta), \tag{14}$$

and, therefore, β can be considered a function of i, p, M_0. Notice from Fig. 2 that the angle of incidence ψ for the central ray on the last reflector is given by

$$2\psi = 2(\alpha + i - p + \beta). \tag{15}$$

This angle ψ can be shown to increase as i is decreased. In the application to be discussed next, a relatively large value for ψ is desirable to allow a frequency diplexer to be used as shown in Fig. 3.

III. AN APPLICATION

As an application, consider the design of an antenna which must transmit at 12 GHz and receive at 14 GHz in a 4.2 m diameter satellite in synchronous orbit at 105° W longitude. Assume a field of view of 3 degrees by 6 degrees (which corresponds approximately to the conti-

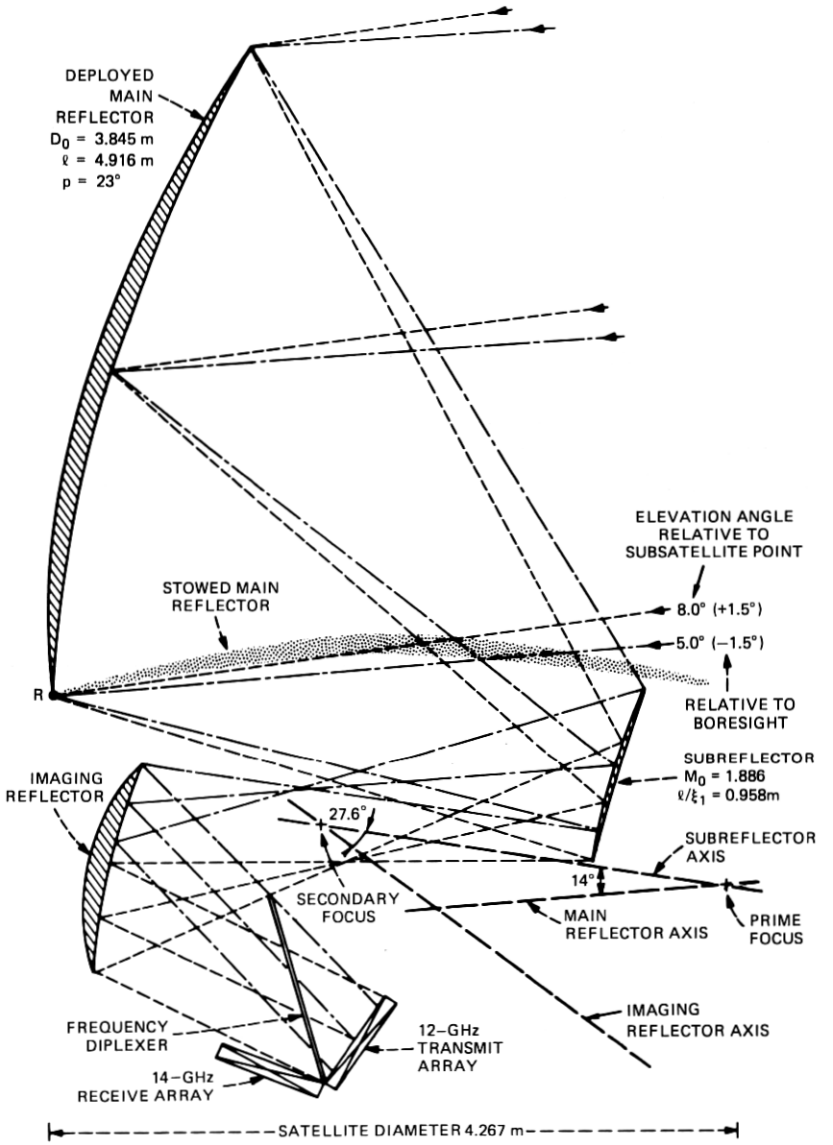

Fig. 3—Imaging satellite antenna with 12/14 GHz frequency diplexing and overall magnification of 7.

nental United States) is required, and suppose separate arrays must be employed for transmission and reception. An arrangement suitable for this purpose is shown in Fig. 3, using a quasi-optical diplexer*

* See, for example Refs. 8 and 9. In Fig. 3, the design requirements are more stringent than in Refs. 8 and 9 because of the wide range of incident angles experienced by the diplexer.

between the two arrays and the last reflector. Figure 4 shows a detail of the feed arrays and diplexer, and Fig. 5 shows a front view of the antenna. The values of M, M_0, etc. are listed in Fig. 3. They were chosen taking into account the requirement that the arrangement should be free of blockage, it should be efficient and, of course, the array should be reasonably small. It is assumed that in Fig. 3 the main reflector can be rotated around R, so that it can be initially stowed in the satellite horizontally as indicated in Fig. 3. Then, once in orbit, it will be rotated into its final position shown in Fig. 3. The size of the main reflector can be increased and still fit in the satellite diameter either by using an elliptical shape or by not stowing the reflector in a completely horizontal position.

Figures 3 and 4 show the paths of the marginal rays in the plane of symmetry for $\delta\theta_0 = \pm 1.5$ degrees. Also shown in Fig. 4 are the rays for $\delta\theta_0 = 0$.

In Section II, the angle $\delta\theta_0$ was assumed to be very small, in which case the illumination over the array aperture can be considered inde-

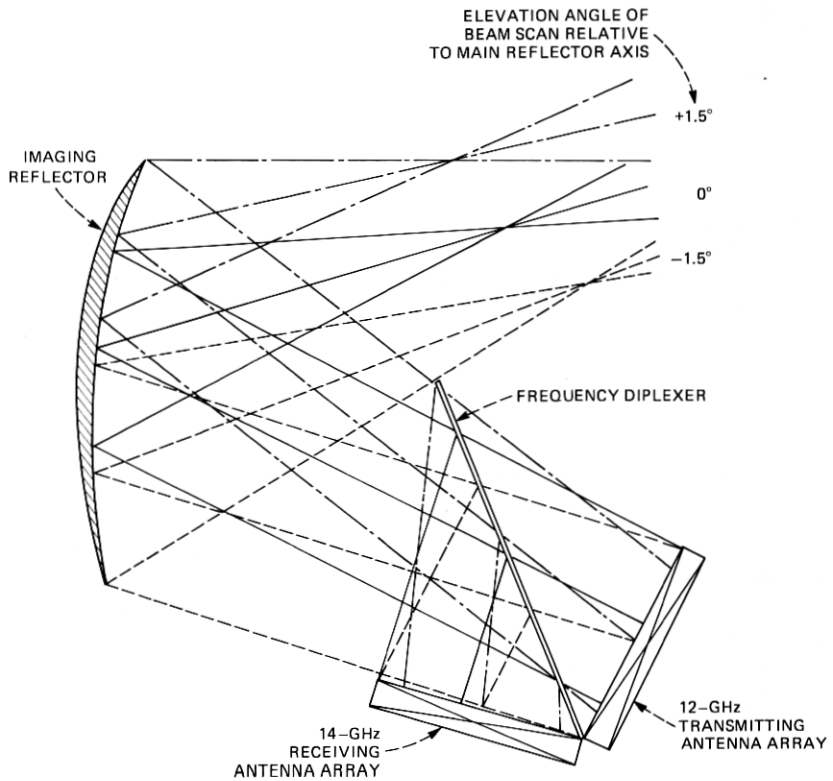

Fig. 4—Detail of feed arrays and diplexer.

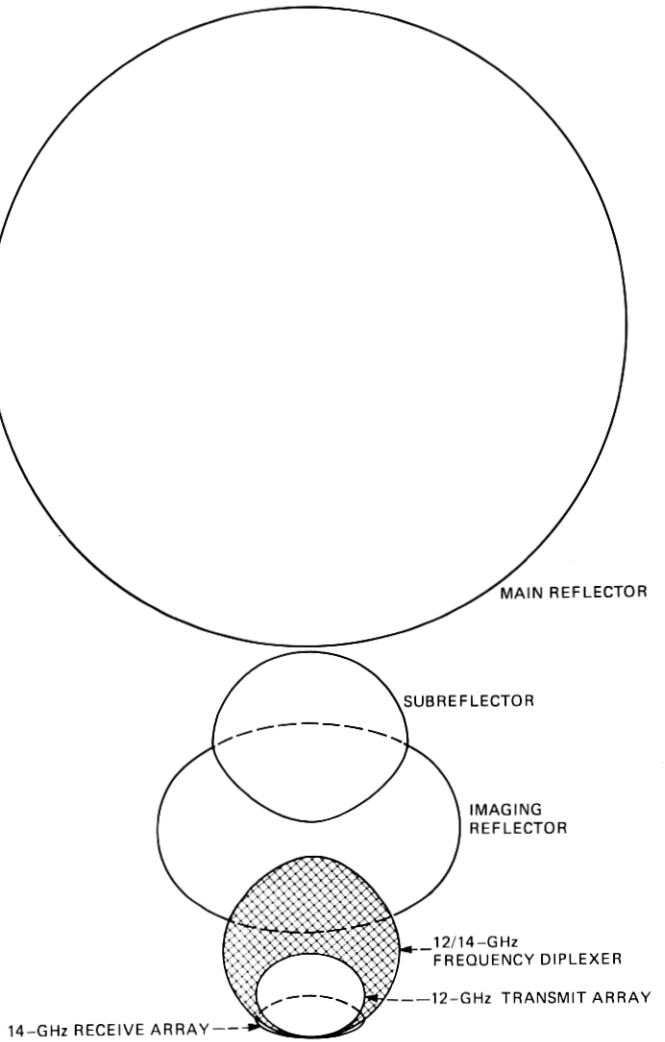

Fig. 5—Front view of imaging satellite antenna.

pendent of $\delta\theta_0$. In the application considered here, however, the angle of incidence $\delta\theta_1$ assumes relatively large values ($\delta\theta_1 = 21$ degrees, for $\delta\theta_0 = 3$ degrees) because of the large magnification $M = 7$. Thus, there is appreciable variation in illumination over the array aperture, and this causes a loss in gain which is now discussed. It is assumed the spacing of the array elements is very small, so that any desired phase distribution over $\sum_1$ can be produced by the array excitation. Then, if g^2 denotes the power distribution on $\sum_1$ due to the array excitation,

the efficiency η of illumination is given by the familiar expression

$$\eta = \frac{\left(\iint_{-\infty}^{\infty} fg\, dx\, dy\right)^2}{\iint_{-\infty}^{\infty} f^2\, dx\, dy \iint_{-\infty}^{\infty} g^2\, dx\, dy}, \tag{16}$$

where $f^2\, dx\, dy$ is the power incident on the element of area $dx\, dy$, caused on $\sum_1$ by a plane wave incident on $\sum_0$. Figure 6 shows for different scan angles the geometric optics array illuminations and the corresponding losses in gain given by eq. (16) for uniform array excitation. Also shown are the losses for a tapered excitation of -10 dB at the edge of the array. Two cases, A and B, are shown in Fig. 6. In case A, the array is centered at C_1 with diameter given by D_0/M. In this case, the scan loss is zero for $\delta\theta_0 = 0$, but it becomes relatively high at the edge of the field of view. In case B, the scan losses for $\delta\theta_0 = \pm 3$ degrees were minimized by increasing the array size and slightly offsetting the array center as shown in Fig. 6 (case B). All losses for -10 dB taper in Fig. 6 are normalized with respect to the value (-0.45 dB taper loss) given by eq. 16 for $\delta\theta_0 = 0$ in case A. This sacrifice in antenna directivity is often made to obtain the sidelobe reduction provided by a -10 dB edge taper.

Curves of scan loss for -10 dB taper in case B are shown in Fig. 7. The positive values near the east and west coasts are due to the above normalization.

IV. CONCLUSIONS

In a conventional reflector antenna, a relatively small feed is usually placed at the focus of a reflector arrangement which then transforms the spherical wave radiated by the feed into a plane wave. In such an antenna, only in part is the power radiated by the feed intercepted by the aperture of the main reflector. Thus, to minimize the loss due to spillover, the edge illumination is usually chosen appreciably lower (-10 dB or less) than the illumination at the center of the aperture. The loss due to spillover is then typically -0.5 dB (in addition to the taper loss mentioned above, giving a total of about -0.9 dB). On the other hand, by using the imaging reflectors and the properly sized and located feed array, less loss is obtained over most of the United States, as shown in Fig. 7. For example, Fig. 7 shows that the loss due to vignetting (i.e., spillover) is largest near the center of the country at a value of -0.6 dB. Losses suffered in the feed array itself are a function of the size and number of feed elements and have not been included.

The imaging arrangements discussed here are particularly useful

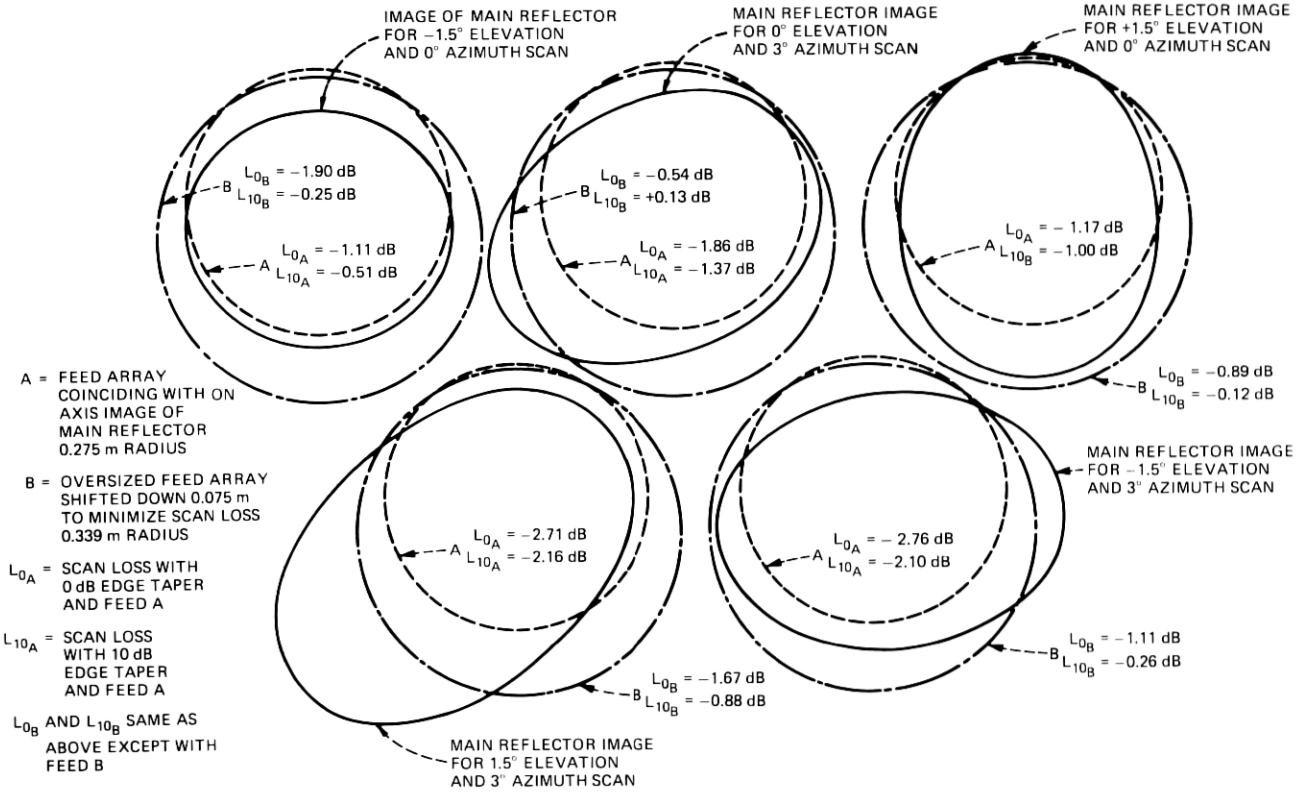

Fig. 6—Vignetting at the array plane for various scan angles.

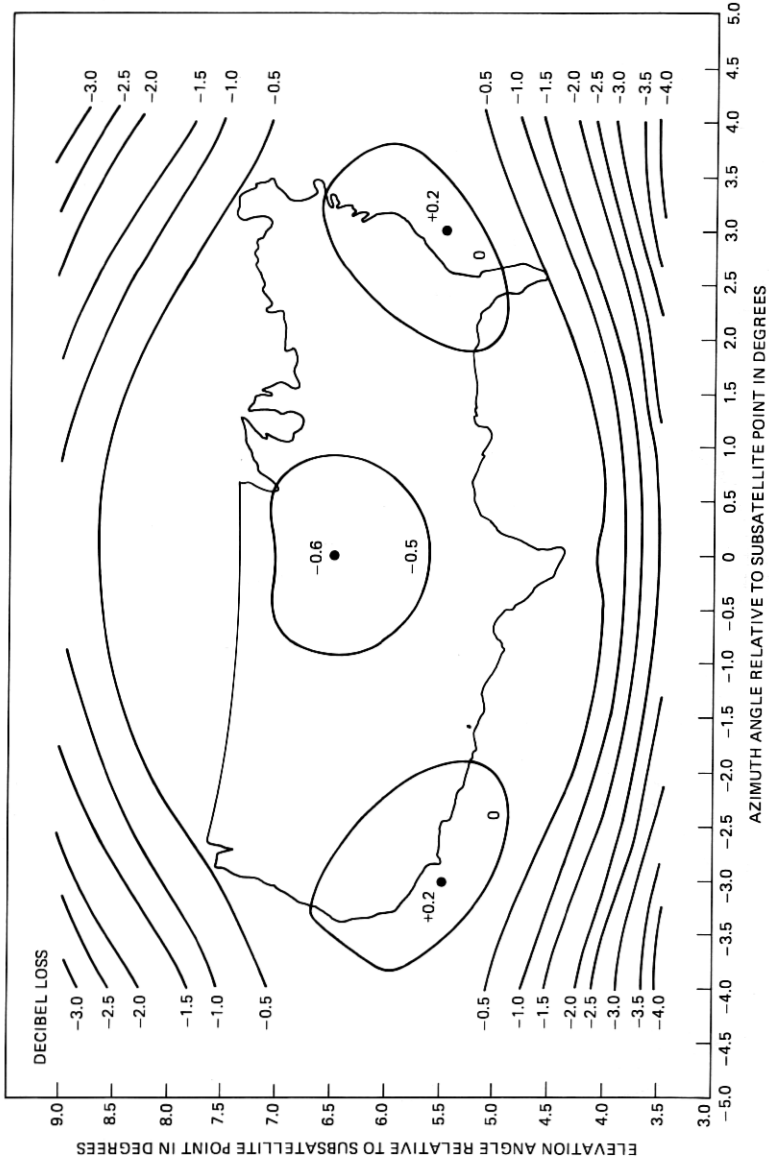

Fig. 7—Contours of scan loss due to imperfect illumination over the array aperture.

when the aperture diameter D_0 is large. The requirements on surface accuracy for the main reflector are greatly reduced because of the ability of the array to correct efficiently for small surface imperfections or reflector displacements. In order for this to work, the array and the reflector must be conjugate elements; i.e., condition (3) is required. This further assures that the transformation relating E_1 to E_0 is essentially frequency independent.

REFERENCES

1. D. O. Reudink and Y. S. Yeh, "A Rapid Scan Area-Coverage Communication Satellite," B.S.T.J., *56,* No. 8 (October 1977), pp. 1549–1561.
2. W. D. Fitzgerald, "Limited Electronic Scanning with an Offset Feed Near-Field Gregorian System," M.I.T. Lincoln Laboratory, Tech. Rep. 486, September 24, 1971, DDC AD-736029.
3. Ming H. Chen and G. N. Tsandoulas, "A Dual-Reflector Optical Feed for Wide-Band Phased Arrays," IEEE Trans. Ant. Prop., *AP-22,* No. 4 (July 1974), pp. 541–545.
4. J. W. Goodman, *Introduction to Fourier Optics,* New York: McGraw-Hill, 1968.
5. C. Dragone, "An Improved Antenna for Microwave Radio Systems Consisting of Two Cylindrical Reflectors and a Corrugated Horn," B.S.T.J., *53,* No. 7 (September 1974), pp. 1351–1377.
6. Hirokawa Tanaka and M. Mizusawa, "Elimination of Cross-Polarization in Offset Dual-Reflector Antennas," Electronics and Communications in Japan, *58-B,* No. 12, 1975.
7. C. Dragone, "Offset Multireflector Antennas with Perfect Pattern Symmetry and Polarization Discrimination," B.S.T.J., *57,* No. 7 (September 1978), pp. 2663–2684.
8. A. A. M. Saleh and R. A. Semplak, "A Qausi-Optical Polarization Independent Diplexer for Use in Beam Feed Systems of Millimeter-Wave Antennas," IEEE Trans. Ant. Prop., *AP-24,* No. 6 (November 1976), pp. 780–784.
9. J. A. Arnaud and F. A. Pelow, "Resonant-Grid Quasi-Optical Diplexers," Elec. Lett., *9,* No. 25 (December 13, 1973), pp. 589–590.